

1 **Rapid age estimation of longnose skate (*Raja rhina*) vertebrae using near infrared**

2 **spectroscopy**

3

4 Morgan B. Arrington^{1*}, Thomas E. Helser², Irina M. Benson², Timothy E. Essington¹, Mary

5 Elizabeth Matta², André E. Punt¹

6

7 ¹School of Aquatic and Fishery Sciences, University of Washington, 1122 Boat Street, Seattle,

8 WA 98195, USA

9 ²Resource Ecology and Fisheries Management Division, Alaska Fisheries Science Center,

10 National Marine Fisheries Service, National Oceanic and Atmospheric Administration, 7600

11 Sand Point Way NE, Seattle, WA 98115, USA

12

13 *corresponding author

14 **Abstract**

15

16 There is a paucity of age data for chondrichthyan fishes due, in large part, to limitations in
17 traditional age estimation methods. Fourier transform near infrared (FT-NIR) spectroscopy has
18 shown promise as an alternative, more efficient method for acquiring age data from
19 chondrichthyans. However, studies are limited to sharks in the Southern Hemisphere. We explored
20 FT-NIR spectroscopy to predict age for a batoid species in the Northern Hemisphere. The longnose
21 skate (*Raja rhina*) is one of a small number of batoids for which annual band periodicity in
22 vertebral centra has been validated, allowing for traditional age estimation and making it an ideal
23 candidate for this study. We fit a multivariate partial least squares predictive model between FT-
24 NIR spectra collected from vertebral centra and traditional age estimates, and tested model
25 predictive skill using external validation. Using FT-NIR spectroscopy, we were able to predict age
26 for longnose skates between the ages of 1 and 14 years with near equal precision and bias as
27 traditional methods in less than a quarter of the time. These results support potential for FT-NIR
28 spectroscopy to increase the amount of age data available for assessments used to inform the
29 conservation and management of this sensitive group of species.

30 1. Introduction

31

32 Information on the age of fishes is an essential component of fisheries research and
33 management. Accurate age data allow for a more robust understanding of population dynamics
34 and contribute to our ability to conserve and manage species effectively (Lai and Gunderson 1987;
35 Campana 2001). Fish age data are essential for age-structured methods of stock assessment as they
36 are used to estimate the size of population cohorts as well as important life-history parameters
37 related to growth, mortality, maturity, and longevity. Because these metrics vary over time,
38 monitoring temporal changes in their values is increasingly recognized as an important component
39 of population assessment. Fish growth can be altered by factors such as ecological and
40 environmental conditions (Shelton and Mangel 2012), fishing mortality (Heino and Dieckmann
41 2008), and density-dependent effects (Lorenzen and Enberg 2001). For example, changes in
42 temperature have been shown to affect fish growth (Matta *et al.* 2010; Pistevos *et al.* 2015; Matta
43 *et al.* 2018), increased mortality can reduce population density leading to increased food
44 availability and faster growth (Heino and Dieckmann 2008), and mortality that is size-selective
45 toward older and larger individuals can favor genotypes that grow faster (Stokes and Law 2000).

46 Despite its importance, monitoring population parameters that rely on age data is
47 challenging because of the time and expense involved, as well as the difficulties with producing
48 reliable age estimates for some vulnerable species such as chondrichthyans. Historically there has
49 not been a large research focus on chondrichthyan species because they have not supported as
50 many economically valuable fisheries as teleost fishes (Fowler *et al.* 2005; Dulvy *et al.* 2014).
51 Additionally, acquiring information on the age of chondrichthyans is especially difficult because
52 they do not possess otoliths, which are commonly used for age estimation of teleost fishes (Cailliet

53 *et al.* 2006; Matta *et al.* 2017). Growth band patterns visible in thin sections of vertebral centra are
54 often used for ageing chondrichthyans, but this method is time consuming and has not been
55 validated for many species (Matta *et al.* 2017). Furthermore, a growing number of studies have
56 demonstrated that these banding patterns may not form annually throughout life in all species,
57 raising doubts about the accuracy of age estimates generated from vertebral centra (Natanson *et*
58 *al.* 2018). Validation across species and age groups using independent methods of age
59 determination is important to ensure that the age-estimation protocol yields biologically accurate
60 age estimates. Consequently, age information is generally lacking for chondrichthyan populations
61 (Cailliet *et al.* 2006; Matta *et al.* 2017) even though many species face elevated risk of extinction
62 due to the expansion of fishing, habitat loss, and climate change (Dulvy *et al.* 2014).

63 The longnose skate (*Raja rhina*) is one of a few species of chondrichthyan for which age
64 estimation methods have been validated (King *et al.* 2017). However, traditional growth-band age
65 estimation is expensive and time consuming for this species, which has precluded routine age
66 estimation. Life history traits such as late age-at-maturity relative to total lifespan and probable
67 low fecundity may make this species more sensitive to exploitation (King and McFarlane 2003),
68 yet a high percentage of bycatch is retained in some areas and there has been interest by industry
69 in developing a target fishery (Farrugia 2017). Thus, more age data would be beneficial to monitor
70 population status with higher spatial and temporal resolution.

71 Fourier transform near infrared (FT-NIR) spectroscopy is a technology that could be used
72 to improve the efficiency of longnose skate age estimation and enable the enhanced collection of
73 age data for this species. Routinely used in pharmaceutical and agricultural industries to analyze
74 chemical composition (McClure *et al.* 2002; Roggo *et al.* 2007), FT-NIR measures the interaction
75 of near-infrared light with the chemistry of biological materials such that unique molecular

76 structures result in a measure of absorbance across a range of wavenumbers from 12,000 to 4,000
77 cm^{-1} (Robins *et al.* 2015). It is being increasingly utilized in ecological research including for
78 species identification, physiological status, sex, detection of disease, and diet composition (Vance
79 *et al.* 2016). In the field of fish ageing, FT-NIR is an emerging technology that has been used to
80 more efficiently estimate ages of teleost fish using otoliths and of sharks using vertebrae, fin
81 spines, and fin clips (Rigby *et al.* 2014; Wedding *et al.* 2014; Robins *et al.* 2015; Rigby *et al.* 2016;
82 Helser *et al.* 2018; Passerotti *et al.* 2020a; Passerotti *et al.* 2020b, Wright *et al.* 2021). The ability
83 to predict animal age using FT-NIR spectroscopy is based on the concept that there is a relationship
84 between an ageing structure's chemical composition and the specimen's age. While this
85 technology has shown promise for estimating chondrichthyan ages, it has not yet been applied to
86 vertebrae in the northern hemisphere or from batoids.

87 Because ages estimated based on annual band periodicity have been validated for longnose
88 skates (King *et al.* 2017), we were presented a unique opportunity to evaluate the use of FT-NIR
89 spectroscopy to estimate ages from the vertebral centra of a batoid species in the northeastern
90 Pacific Ocean. The objective of this study is to evaluate the utility of FT-NIR spectroscopy to
91 estimate longnose skate age and compare results relative to traditional methods.

92

93 **2. Materials and methods**

94

95 The longnose skate vertebral centra used in this study were provided by the National
96 Marine Fisheries Service (NMFS) Northwest Fisheries Science Center's (NWFSC) bottom trawl
97 research surveys (Keller *et al.* 2017). A segment of thoracic vertebrae was collected from
98 specimens and frozen at sea following approved NMFS procedures and guidance from the NMFS

99 Animal Care and Use Policy (Policy Directive 04-112). Collections occurred during 2011-2012
100 along the U.S. West Coast between May and October. These samples were processed for a separate
101 study on regional variability in the age and growth of longnose skates and more details and sample
102 collection locations are fully described in Arrington (2020). A group of three to four adjacent
103 thoracic vertebrae were dissected out of the frozen vertebral column in the laboratory, neural and
104 hemal arches were removed, and centra were stored in ethanol for preservation (Cailliet and
105 Goldman 2004). One centrum per specimen was used for age estimation and another one was used
106 for spectroscopic evaluation in this study. Age readers estimated ages by counting annually
107 deposited growth bands on vertebral thin sections according to the validated protocol (Gburski *et*
108 *al.* 2007; King *et al.* 2017). Hereinafter, we refer to reader-generated age estimates as “traditional
109 ages”, while “predicted ages” represent the ages estimated using the calibration model in the FT-
110 NIR spectroscopy approach. The primary reader (Reader 1) aged all specimens. Then, to evaluate
111 ageing error, two additional readers independently aged a random subset of vertebral thin sections.
112 We only evaluated a single vertebra per individual to maximize the number of individuals, but
113 future studies might explore variation in growth across vertebrae within individuals. Traditional
114 age estimates from the full longnose skate dataset ranged from 0 to 19 years (Arrington 2020). For
115 the purpose of the present study, we truncated the dataset at 14 years due to poor representation of
116 the older age classes (fewer than 5 samples per age class), which could have a disproportionately
117 large influence on the predictive model.

118 To collect FT-NIR spectral absorbance data (hereinafter called spectral data), we placed
119 one whole centrum per specimen under a fume hood and allowed it to air-dry for 48 hours so that
120 ethanol could fully evaporate. We then placed each centrum on the sampling window of a Bruker
121 TANGO-R Fourier transform near infrared spectrometer (Bruker Optics, Ettlingen, Germany) in

122 a standardized orientation with centrum cone side down and covered it with a reflector cap.
123 Spectral data were acquired at 16 cm^{-1} resolution with 64 co-added scans. We collected spectral
124 data from 633 vertebrae (Fig. 1a).

125 Partial Least Squares (PLS) regression analysis was used to build a predictive model for
126 longnose skate age based on spectral data of whole centra. A PLS regression is a multivariate
127 regression method commonly used for chemometric analysis (Wold *et al.* 1984). In PLS, the
128 independent (here, spectral data) and dependent (here, Reader 1's traditional age estimate) data
129 matrices are decomposed into a set of scores and loadings. Loadings are determined by maximizing
130 the correlation between scores based on least squares. We conducted data analysis in R statistical
131 computing software version 3.6.3 (R Core Team 2020), with chemometric packages *mdatools*
132 (Kucheryavskiy 2020) and *simplerspec* (Baumann 2020).

133 Raw spectral data often need to be transformed to enhance variation between specimens
134 and remove unwanted noise before modeling (Rinnan *et al.* 2009). First, we estimated the first
135 derivative of the spectral data to enhance separation between spectra while reducing any baseline
136 drift in the data (Brown *et al.* 2000). We calculated the first derivative using a polynomial least
137 squares estimation known as the Savitzky-Golay first derivative (17-point smooth, polynomial
138 order = 1; Savitzky and Golay 1964). The Savitzky-Golay approach is commonly used in
139 spectroscopy due to desirable properties such as reducing unwanted noise in spectral data while
140 preserving the chemical signal of interest. After calculating the first derivative, we mean centered
141 the data (Fig. 1b). We then split the data into a set used to calibrate the model and a set to externally
142 validate it. These sets were selected so that the validation set contained all specimens that each had
143 three independent traditional age estimates. This allowed us to directly compare ageing error
144 between the FT-NIR spectroscopy approach and the traditional method. The calibration set

145 contained 413 samples and the validation set contained 220 samples (Fig. 2). We applied PLS to
146 the pre-processed spectral data from the calibration set and Reader 1's corresponding traditional
147 age estimates using a 10-fold venetian blind cross validation. This is a version of k-fold cross
148 validation in which each fold is constructed from samples in the dataset in the 1 through 10 position
149 until all data have been sorted. Each fold is systematically left out and a PLS regression is applied
150 to the remaining samples. The parameter estimates are then used to estimate the age of the left-out
151 fold and the mean error of all predictions versus Reader 1's estimated ages can be calculated as
152 the root mean square error of cross validation (RMSECV). This is an estimate of the predictive
153 ability of the model on new data. We then applied this model to the validation data set and
154 calculated a root mean square error of prediction (RMSEP) between predicted and Reader 1's
155 traditional age estimates to measure the true predictive ability of the model on an external data set.
156 We also report percentage root mean square error ($\% \text{ RMSE} = (\text{RMSECV}/\text{maximum age} \times 100)$)
157 to estimate the average predictive ability of the PLS model within the range of the age data
158 (Couture *et al.* 2016; Passerotti *et al.* 2020a). This metric also provides a standardized measure of
159 error that can be compared across studies (Passerotti *et al.* 2020a).

160 Lastly, we assessed age estimation error in the FT-NIR spectroscopy approach compared
161 to the traditional method. There are two types of error associated with traditional age and growth
162 studies: process error and observation error. Process error occurs when growth zones in the ageing
163 structure do not reflect true age. We did not address process error in this study. However, King *et*
164 *al.* (2017) suggest annual band periodicity in the vertebrae of longnose skates. Observation error
165 is due to interpretation of the ageing structure and can be evaluated by comparing age estimates
166 among multiple age readers. In the FT-NIR approach, we considered observation error to be error
167 between FT-NIR predicted age and Reader 1's traditional age estimates.. This definition of

168 observation error is based on the simplifying assumption that there is no process error in FT-NIR
169 measurements that would result in different age estimates for the same specimens, though this has
170 yet to be evaluated or quantified for this species. To evaluate the precision of each method, we
171 compared the coefficient of variation (CV) between Reader 1's traditional age estimates and the
172 FT-NIR predicted ages to the CV among the three age reader estimates (Chang 1982). McBride
173 (2015) found that CV tracks precision better than other commonly used measures, such as average
174 percent agreement (APE). We evaluated relative bias among traditional methods and the FT-NIR
175 approach visually using age bias plots and Bowker's test of symmetry (Hoenig *et al.* 1995;
176 McBride 2015). Since the PLS regression returns fractional age estimates, we first had to round
177 predictions to the nearest whole number (i.e. 2.45 years = 2 years) so that precision and relative
178 bias could be compared between the two methods. We evaluated current levels of observation error
179 based on precision and relative bias among traditional age estimates to compare to the performance
180 of the FT-NIR approach and to evaluate the utility of this approach for generating age estimates
181 for longnose skates.

182

183 **3. Results**

184

185 The FT-NIR spectra of longnose skate vertebral centra correlated with Reader 1's
186 traditionally estimated age with a coefficient of determination (R^2) of 0.86, a RMSECV of 1.38
187 years, and a %RMSE of 9.87% (Fig. 3). The RMSECV of 1.38 years indicates that 67% of the
188 predicted ages from cross-validation fell within 1.38 years of the traditionally estimated age. When
189 the model was applied to the external validation set and predictions compared to Reader 1's
190 traditional age estimates, RMSEP was 1.32 years (Fig. 3).

191 The FT-NIR approach predicted longnose skate ages between 1 and 14 years in the external
192 validation set with as much precision as the traditional method but with a slight increase in bias
193 for individuals at either end of the age range. Specimens with Reader 1's traditional age estimate
194 of 0 years were imprecisely estimated by the PLS regression (Fig. 3). When age-0 specimens were
195 included, the traditional method had a CV of 22.6% among the three age readers and no systematic
196 disagreement between Reader 1 and 2 (Bowker's $\chi^2 = 32.10$, d.f. = 29, $P = 0.315$) or Reader 1 and
197 3 (Bowker's $\chi^2 = 46.91$, d.f. = 40, $P = 0.210$). Precision was lower between the FT-NIR predictions
198 and the Reader 1's traditional age estimates with a CV of 34.2% and the null hypothesis of no
199 systematic disagreement between methods was rejected (Bowker's $\chi^2 = 61.06$, d.f. = 37, $P = 0.008$).
200 When specimens with Reader 1's traditional age estimate of 0 were removed, the precision
201 between FT-NIR predictions and Reader 1's traditional age estimates (CV of 19.6%) was
202 comparable to that among readers (CV of 19.1%) and Bowker's test of symmetry indicated no
203 systematic disagreement between methods (Bowker's $\chi^2 = 42.86$, d.f. = 35, $P = 0.170$). We visually
204 observed a slight bias in FT-NIR predictions, with a tendency to over-estimate the age of younger
205 skates (< 2 years) and under-estimate the age of older skates (> 13 years) relative to the three age
206 reader estimates (Fig. 4). When the magnitude of discrepancies in age estimates was compared
207 between traditional and FT-NIR spectroscopy methods, we found that the percentage of samples
208 with complete agreement (discrepancy of 0 years) was slightly higher among age readers using
209 traditional methods (41.5–45.1% agreement) than between Reader 1's estimates and FT-NIR
210 predictions (33.0% agreement), but otherwise had a similar distribution (Fig. 5).

211

212 **4. Discussion**

213

214 The results of this study suggest that FT-NIR spectra of longnose skate centra can be used
215 to estimate skate ages, similar to results published for other chondrichthyan species (Rigby *et al.*
216 2014; Rigby *et al.* 2016). When applied to an external validation set, the FT-NIR spectroscopy
217 method produced age predictions with comparable precision to traditional methods for longnose
218 skates between the ages of 1 and 14 years (the full age range in this study was 0-14). Since the
219 traditional method has been shown to produce biologically accurate age estimates (King *et al.*
220 2017), these findings support the validity of using FT-NIR predicted ages in age-based assessments
221 of longnose skates. Additionally, this method provides considerable efficiency gains -- a scan takes
222 just one minute and requires minimal preparation of the sample. Traditional methods for longnose
223 skate age determination require extensive preparation and take between 15 and 30 minutes per
224 sample. Estimates can also be biased among age readers, especially among different agencies
225 (King *et al.* 2017). FT-NIR spectroscopy may allow age estimation to be standardized among age
226 readers and agencies due to its reproducibility. This technology has the potential to improve the
227 frequency, quantity, and reproducibility of longnose skate age data for use in stock assessments
228 and management.

229 This study marks the first known application of this technology to a batoid and results were
230 comparable to those found by Rigby *et al.* (2014, 2016) for shark vertebrae. For *Sphyrna*
231 *mokarran*, *Carcharhinus sorrah*, and *Squalus megalops*, Rigby *et al.* (2014, 2016) developed
232 calibration models that yielded R^2 values between 0.78 and 0.89, RMSECV values of 1.23 to 2.48
233 years, and uncertainty between 7 and 9% (%RMSE of 7.40 to 8.97). The FT-NIR spectroscopy
234 analysis of longnose skate vertebrae in this study produced comparable calibration models with an
235 R^2 of 0.86, RMSECV of 1.38 years, and uncertainty of 9.87% (Fig. 3).

236 The biased age predictions we observed for age-0 longnose skates in the external validation
237 relative to traditional methods could be due to the exceedingly small size of age-0 vertebrae (1.5
238 mm). Passerotti *et al.* (2020b) hypothesized that excess stray light from the FT-NIR spectrometer
239 might confound their results for otoliths of juvenile red snapper that were between 1.5 and 7.0 mm.
240 They found better calibration models when using a Teflon aperture to constrain the field of light.
241 Future work for longnose skates could include using an aperture that may improve the predictive
242 ability of the FT-NIR spectroscopy approach for younger skates.

243 Except for age 0 skates, the FT-NIR spectroscopy approach yielded age predictions for the
244 external validation set that had comparable precision to the traditional method currently used for
245 production ageing. However, neither method was as precise as is typical for teleost age
246 determination. Poor precision in age estimation is common for chondrichthyan species due to the
247 difficulty of interpreting their ageing structures. Published CVs for chondrichthyan vertebrae are
248 generally much higher (>10%) than those for teleost otoliths (~5%) (Campana 2001). The current
249 study reports slightly poorer precision in the traditional method (CV = 19.1%) than prior ageing
250 studies for longnose skates by Thompson (2006), Gburski *et al.* (2017), and King *et al.* (2017) that
251 found CVs between 11.9% and 15.2%. However, this is likely due to the large number of young
252 skates included in the current study. It is difficult to distinguish growth increments on longnose
253 skate vertebrae under the age of 2 years and any disagreement within this age range is weighed
254 more heavily in the calculation of the overall CV. For instance, when one reader assigns an age of
255 0 and another assigns an age of 1 to a given individual, the disagreement dramatically inflates the
256 CV.

257 The low precision of traditional age estimates in this study relative to teleosts is likely due
258 to observation error. However, the equivalently low precision of FT-NIR predictions could be due

259 to several factors. First, any observation error associated with the traditional age estimates used
260 to calibrate the model could reduce the precision of age predictions. Second, some process error is
261 likely present in vertebrae which could cause a difference in the visual versus spectral
262 interpretation of the structure. Third, any natural variation in chemical composition of vertebrae
263 may affect the spectral data collected using FT-NIR spectroscopy. This may be amplified because
264 we were unable to standardize the exact position of the thoracic vertebral samples used for
265 spectroscopy. Size of vertebrae is variable along the vertebral column, and it is possible that larger
266 thoracic vertebrae could impart different FT-NIR spectra than smaller thoracic vertebrae within an
267 individual. Finally, the calibration model did not contain as many older skates as young skates,
268 which could affect its predicative capability in that age range. Ideally, calibration samples would
269 have even representation from all age classes. Rigby *et al.* (2014) found that age predictions
270 markedly improved when older age classes were better represented in the calibration model.

271 An increasing number of studies show that vertebral banding patterns may not form
272 annually throughout life in all species (Natanson *et al.* 2018). This finding raises doubts about the
273 accuracy of age estimates from vertebral centra in general and suggests that process error may be
274 common. However, Rigby *et al.* (2014) found FT-NIR to be a promising alternative method for
275 estimating age from vertebrae even when no visible banding pattern is present. Rigby *et al.* (2016)
276 also found that using known-age samples to build predictive models based on FT-NIR spectra had
277 improved precision relative to using traditionally estimated ages with RMSECV of +/- less than a
278 year (0.87 and 0.88 years). This demonstrates the potential for FT-NIR spectroscopy to estimate
279 age despite process error if accurate ages are used to calibrate the model. These findings indicate
280 that as the accuracy and representation of age estimates used to calibrate the model improve, we
281 may be able to improve the precision of age predictions. Future work for longnose skates could

282 include using a more balanced dataset to fit the calibration model between spectra and age
283 estimates, utilizing known-age specimens, and standardizing the position of centra along the
284 vertebral column. This may help to resolve bias in younger and older ages and improve precision
285 while also improving the accuracy of age estimates.

286 The results of this study as well as those of Rigby *et al.* (2014, 2016) indicate that there is
287 a correlation between age and the chemical composition of vertebrae. It is unknown what specific
288 chemical compound(s) correlate with age in chondrichthyans, but it could be related to the quantity
289 of calcified phosphate mineral, hydroxyapatite, in their cartilaginous vertebral centra, as
290 mineralization occurs incrementally with age in many chondrichthyans (Cailliet 1990; Kerr and
291 Campana 2014). Calcium hydroxyapatite is detectable in the NIR spectrum due to stretching and
292 bending of OH bonds in surface hydroxyl groups when exposed to near infrared light (Elkabouss
293 *et al.* 2004). Relative quantities of the unmineralized components of vertebrae may also contribute
294 to the observed relationship between NIR spectra and age. The unmineralized components of
295 chondrichthyan vertebrae include water, proteoglycan, and collagen fibers, which are also
296 detectable in the NIR region between 5,400 and 3,800 cm^{-1} (Baykal *et al.* 2010). Future work is
297 needed to determine the specific chemistry of chondrichthyan vertebrae related to age to better
298 understand the mechanism driving the observed correlation between age and FT-NIR spectra.

299 The results of this study show promise for the use of FT-NIR spectroscopy to more rapidly
300 and efficiently estimate ages for longnose skates. The FT-NIR approach provides considerable
301 efficiencies over the labor-intensive traditional process of preparing vertebrae for age
302 determination. This is important because it may allow for a larger quantity and higher frequency
303 of age estimates to be generated for use in stock assessments to monitor the status of this species.
304 Additionally, modern stock assessment software allows the inclusion of ageing error in population

305 models and the results of this study provide the basis for quantifying this error. The most recent
306 assessment for longnose skate off the US West Coast included age-reading error matrices
307 estimated using the approach of Punt et al. (2008) based on various models of the relationship
308 between the CV of age-reading error and true age (Gertseva *et al.* 2019). This study also adds to a
309 growing body of literature demonstrating the successful application of this technology to estimate
310 age for chondrichthyan species. Fourier transform near infrared spectroscopy may provide a way
311 to estimate age for other members of this sensitive group of fishes that previously had little to no
312 age data available.

313

314 **Acknowledgments**

315 We thank the vessel crews from the National Marine Fisheries Service's (NFMS) bottom trawl
316 surveys for providing vertebrae samples. Many thanks to Christopher Gburski for generously
317 assisting with this study by providing training, age estimates, and logistical support. We thank
318 project interns Emma Evans and Melinda Carr for wonderful assistance with sample preparation
319 and processing. Olav Ormseth, Brenna Groom, and two anonymous reviewers provided helpful
320 reviews that improved this manuscript. Fish research by the National Marine Fisheries Service is
321 not required to undergo ethical review as per the National Marine Fisheries Service Animal Care
322 and Use Policy (Policy Directive 04-112). This policy (04-112) is currently limited to research
323 on free-living marine mammals, seabirds, and sea turtles and does not cover research on captive
324 or wild fish. However, fish samples used in this study were considered dead in the net upon
325 arrival on board and collected and handled in strict accordance within the guidelines of the U.S.
326 Government Principles for the Utilization and Care of Vertebrate Animals Used in Testing,
327 Research and Training and the American Fisheries Society Guidelines for the Use of Fishes in

328 Research (https://fisheries.org/docs/policy_useoffishes.pdf; Chapter V). Permits acquired for
329 sample collection including NOAA, NMFS, WCR (West Coast Region) Scientific Research
330 Permit 2011: SRP-06-2011 and 2012: SRP-06-2012, Oregon Scientific Taking Permit for Fish
331 and Marine and Freshwater Invertebrates: 2011: Permit 16328 and 2012: Permit 17200, CA
332 Scientific Collecting Permit from the California Department of Fish and Game for 2011-2013:
333 SC-11678, National Marine Sanctuary Permit for 2010 -2012: Multi-2010-004. The authors
334 thank Aimee Keller for providing permit information. This research was supported by a grant
335 from the NOAA Fisheries Office of Science and Technology's Improve a Stock Assessment
336 program and a graduate fellowship from the University of Washington's School of Aquatic and
337 Fishery Sciences. The scientific results and conclusions, as well as any views or opinions are
338 those of the author(s) and do not necessarily reflect those of NOAA or the Department of
339 Commerce. Reference to trade names does not imply endorsement by the National Marine
340 Fisheries Service, NOAA.

341

342

343 **Conflicts of Interest**

344 The authors declare no conflicts of interest.

345

346 **Data Availability Statement**

347 The data that support this study will be shared upon reasonable request to the corresponding
348 author. More information available at <https://www.fisheries.noaa.gov/resource/data/age-and-growth-otolith-collections-ageing-methods>.
349

350

351 **References**

- 352 Arrington, M. B. (2020). Growth and maturity of Longnose Skates (*Raja rhina*) along the North
353 American West Coast. M.Sc. Thesis, University of Washington, Seattle, WA.
- 354 Baykal, D., Irrechukwu, O., Lin, P., Fritton, K., Spencer, R. G., and Pleshko, N. (2010).
355 Nondestructive assessment of engineered cartilage constructs using near-infrared spectroscopy.
356 *Applied Spectroscopy* **64**, 1160-1166.
- 357 Baumann, P. (2020). *simplerspec: Soil and plant spectroscopic model building and prediction. R*
358 *package version 0.1.0.9001*. Available at <https://github.com/philipp-baumann/simplerspec>.
- 359 Brown, C. D., Vega-Montoto, L., and Wentzell, P. D. (2000). Derivative preprocessing and
360 optimal corrections for baseline drift in multivariate calibration. *Applied Spectroscopy* **54**, 1055-
361 1068.
- 362 Cailliet, G. M. (1990). Elasmobranch age determination and verification: an updated review, pp.
363 157–165. In H. L. Pratt, S. H. Gruber, and T. Taniuchi (eds.), *Elasmobranchs as Living*
364 *Resources: Advances in the Biology, Ecology, Systematics, and the Status of the Fisheries*.
365 *Proceedings of the Second United States–Japan Workshop, 9–14 December 1987, Honolulu, HI,*
366 *USA*. U.S. Department of Commerce, NOAA Technical Report NMFS 90.
- 367 Cailliet, G. M., and Goldman, K. J. (2004). Age determination and validation in Chondrichthyan
368 fishes. Pages 399-447 in J. C. Carrier, J. A. Musick, and M. R. Heithaus, editors. *Biology of*
369 *Sharks and Their Relatives*. CRC Press, Boca Raton, FL.

- 370 Cailliet, G. M., Smith, W. D., Mollet, H. F. and Goldman, K. J. (2006). Age and growth studies
 371 of chondrichthyan fishes: the Need for consistency in terminology, verification, validation, and
 372 growth function fitting. *Environmental Biology of Fishes* **77**, 211-228.
- 373 Campana, S. E. (2001). Accuracy, precision and quality control in age determination, including a
 374 review of the use and abuse of age validation methods. *Journal of Fish Biology* **59**, 197-242.
- 375 Chang, W.Y.B. (1982). A statistical method for evaluating the reproducibility of age
 376 determination. *Canadian Journal of Fisheries and Aquatic Sciences* **39**, 1208-1210.
- 377 Couture, J. J., Singh, A., Rubert-Nason, K. F., Serbin, S. P., Lindroth, R. L., and Townsend, P.
 378 A. (2016). Spectroscopic determination of ecologically relevant plant secondary metabolites.
 379 *Methods in Ecology and Evolution* **7**, 1402-1412.
- 380 Dulvy, N. K., Fowler, S. L., Musick, J. A., Cavanagh, R. D., Kyne, P. M., Harrison, L. R.,
 381 Carlson, J. K., Davidson, L., Fordham, S. V., Francis, M. P., Pollock, C. M., Simpfendorfer, C.
 382 A, Burgess, G. H., Carpenter, K. E., Compagno, L., Ebert, D. A., Gibson, C., Heupel, M. R.,
 383 Livingstone, S. R., Sanciangco, J. C., Stevens, J. D., Valenti, S., and White, W. T. (2014).
 384 Extinction risk and conservation of the world's sharks and rays. *eLife* **3**, 1-34.
- 385 Elkabouss, K., Kacimi, M., Ziyad, M., Ammar, S. and Bozon-Verduraz, F. (2004). Cobalt-
 386 exchanged hydroxyapatite catalysts: Magnetic studies, spectroscopic investigations, performance
 387 in 2-butanol and ethane oxidative dehydrogenations. *Journal of Catalysis* **226**, 16-24.
- 388 Farrugia, T. J. (2017). Interdisciplinary assessment of the skate fishery in the Gulf of Alaska.
 389 Ph.D. Diss., University of Alaska Fairbanks, Fairbanks, AK.

RAPID AGE ESTIMATION OF LONGNOSE SKATE VERTEBRAE

- 390 Fowler, S. L., Cavanagh, R. D., Camhi, M., Burgess, G. H., Cailliet, G. M., Fordham, S.V.,
391 Simpfendorfer, C. A., and Musick, J.A. (2005). Sharks, Rays and Chimaeras: The Status of the
392 Chondrichthyan Fishes. IUCN/SSC Shark Specialist Group. IUCN, Gland, Switzerland and
393 Cambridge, UK.
- 394 Gertseva, V. Matson, S., Taylor, I. Bizzarro, J, Wallace, J. (2019). Stock assessment of the
395 Longnose Skate (*Beringraja rhina*) in state and Federal waters off California, Oregon and
396 Washington. Pacific Fishery Management Council, Portland, OR.
- 397 Gburski, C.M., Gaichas, S.K., and Kimura, D.K. (2007). Age and growth of Big Skate (*Raja*
398 *binoculata*) and Longnose Skate (*R. rhina*) in the Gulf of Alaska. *Environmental Biology of*
399 *Fishes* **80**, 337-349.
- 400 Heino, M. and Dieckmann, U. (2008). Detecting fisheries-induced life-history evolution: an
401 overview of the reaction-norm approach. *Bulletin of Marine Science* **83**, 69-93.
- 402 Helser, T. E., Benson, I., Erickson, J., Healy, J., Kastle, C., and Short, J.A. (2018). A
403 transformative approach to ageing fish otoliths using Fourier transform near infrared
404 spectroscopy: a Case study of eastern Bering Sea walleye pollock (*Gadus chalcogrammus*).
405 *Canadian Journal of Fisheries and Aquatic Sciences* **76**, 1-10.
- 406 Hoenig, J. M., Morgan, M. J., and Brown, C. A. (1995). Analysing differences between two age
407 determination methods by tests of symmetry. *Canadian Journal of Fisheries and Aquatic*
408 *Sciences* **52**, 364-368.

- 409 Keller, A. K., Wallace, J. R., Methot, R. D. (2017). The Northwest Fisheries Science Center's
410 West Coast Groundfish Bottom Trawl Survey: History, Design, and Description. U.S.
411 Department of Commerce, NOAA Technical Memorandum NMFS-NWFSC-136.
- 412 Kerr, L.A., and Campana, S.E. (2014). Chemical composition of fish hard parts as a natural
413 marker of fish stocks. Pages 205-234 in S. X. Cadrin, L. A. Kerr, and S. Mariani, editors. Stock
414 Identification Methods 2nd Edition. Academic Press, San Diego.
- 415 King, J. R., and McFarlane, G. A. (2003). Marine fish life history strategies: Applications to
416 fishery management. *Fisheries Management and Ecology* **10**, 249-264.
- 417 King, J. R., Helser, T., Gburski, C., Ebert, D. A., Cailliet, G., and Kestelle, C. R. (2017). Bomb
418 radiocarbon analyses validate and inform age determination of Longnose Skate (*Raja rhina*) and
419 Big Skate (*Beringraja binoculata*) in the North Pacific Ocean. *Fisheries Research* **193**, 195-206.
- 420 Kucheryavskiy, S. (2020). mdatools - R package for chemometrics. Chemometrics and
421 Intelligent Laboratory Systems. Available at <https://doi.org/10.1016/j.chemolab.2020.103937>.
- 422 Lai, H. L., and Gunderson, D. R. (1987). Effects of ageing errors on estimates of growth,
423 mortality and yield per recruit for walleye pollock (*Theragra chalcogramma*). *Fisheries*
424 *Research* **5**, 287-302.
- 425 Lorenzen, K., and Enberg, K. (2002). Density-dependent growth as a key mechanism in the
426 regulation of fish populations: evidence from among-population comparisons. *Proceedings of the*
427 *Royal Society B: Biological Sciences* **269**, 49-54.

- 428 Matta, M.E, Black, B.A, and Wilderbuer, T.K. (2010). Climate-driven synchrony in otolith
 429 growth-increment chronologies for three Bering Sea flatfish species. *Marine Ecology Progress*
 430 *Series* **413**, 137-145.
- 431 Matta, M.E., Tribuzio, C. A., Ebert, D. A., Goldman, K. J., and Gburski, C. M. (2017). Age and
 432 growth of elasmobranchs and applications to fisheries management and conservation in the
 433 Northeast Pacific Ocean. *Advances in Marine Biology* **77**, 179-220.
- 434 Matta, M. E., Helser, T. E., and Black, B. A. (2018). Intrinsic and environmental drivers of
 435 growth in an Alaskan rockfish: an Otolith biochronology approach. *Environmental Biology of*
 436 *Fishes* **101**, 1571-1587.
- 437 McClure, W., Crowell, B., Stanfield, D., Mohapatra, S., Morimoto, S., and Batten, G. (2002).
 438 Near infrared technology for precision environmental measurements: Part 1. Determination of
 439 nitrogen in green-and dry-grass tissue. *Journal of Near Infrared Spectroscopy* **10**, 177-185.
- 440 McBride, R. (2015). Diagnosis of paired age agreement: a simulation of accuracy and precision
 441 effects. *ICES Journal of Marine Science* **72**, 2149-2167.
- 442 Natanson, L. J., Skomal, G. B., Hoffman, S. L., Porter, M. E., Goldman, K. J., and Serra, D.
 443 (2018). Age and growth of sharks: Do vertebral band pairs record age? *Marine Freshwater*
 444 *Research* **69**, 1440-1452.
- 445 Passerotti, M. S., Helser, T. E., Benson, I. M., Barnett, B. K., Ballenger, J. C., Bubley, W. J.,
 446 Reichert, M. J. M., and Quattro, J. M. (2020a). Age estimation of Red Snapper (*Lutjanus*
 447 *campechanus*) using FT-NIR spectroscopy: Feasibility of application to production ageing for
 448 management. *ICES Journal of Marine Science* **77**, 2144–2156.

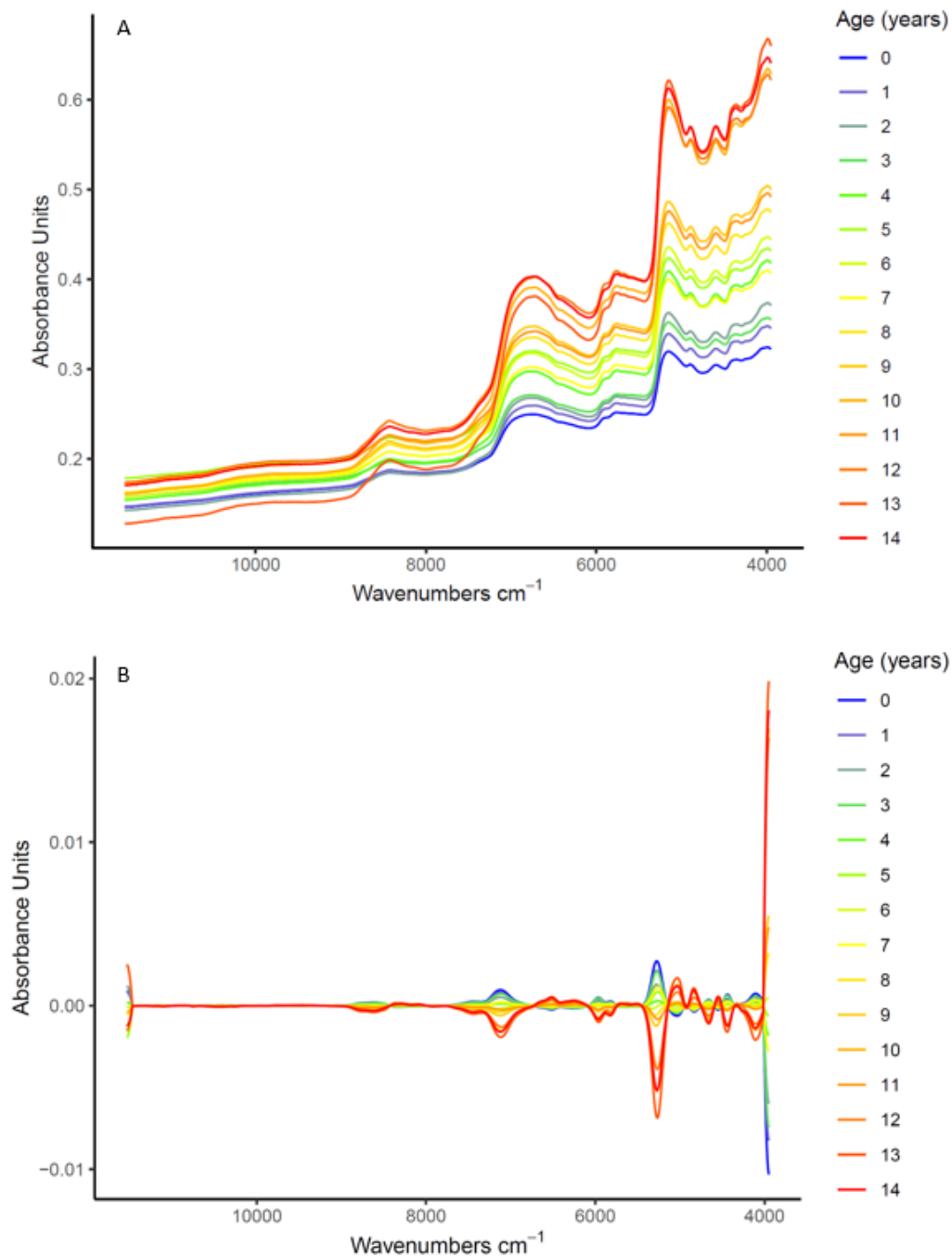
- 449 Passerotti, M. S., Jones, C. M., Swanson, C. E., and Quattro, J. M. (2020b). Fourier-transform
 450 near infrared spectroscopy (FT-NIRS) rapidly and non-destructively predicts daily age and
 451 growth in otoliths of juvenile red snapper *Lutjanus campechanus* (Poey, 1860). *Fisheries*
 452 *Research* **223**, 1-8.
- 453 Pistevos, J. C. A., Nagelkerken, I., Rossi, T., Olmos, M., and Connell, S. D. (2015). Ocean
 454 acidification and global warming impair shark hunting behaviour and growth. *Scientific Reports*
 455 **5**, 1-10.
- 456 Punt, A. E., Smith, D. C., KrusicGolub, K., Roberston, S. (2008). Quantifying age-reading error
 457 for use in fisheries stock assessments, with application to species in Australia's southern and
 458 eastern scalefish and shark fishery. *Canadian Journal of Fisheries and Aquatic Sciences* **65**,
 459 1991-2005.
- 460 R Core Team (2020). *R: A Language and Environment for Statistical Computing*, Vienna,
 461 Austria. Available at: <https://www.R-project.org/>.
- 462 Rigby, C.L., Wedding, B. B., Grauf, S., and Simpfendorfer, C. A. (2014). The utility of near
 463 infrared spectroscopy for age estimation of deepwater sharks. *Deep-sea Research Part I:*
 464 *Oceanographic Research Papers* **94**, 184-194.
- 465 Rigby, C. L., Wedding, B. B., S. Grauf, and Simpfendorfer, C. A. (2016). Novel method for
 466 shark age estimation using near infrared spectroscopy. *Marine and Freshwater Research* **67**,
 467 537- 545.
- 468 Rinnan, A., van den Berg, F., Engelsens, S. B. (2009). Review of the most common pre-
 469 processing techniques for near-infrared spectra. *Trends in Analytical Chemistry* **28**, 1201-1222.

- 470 Robins, J. B., Wedding, B. B., Wright, C., Grauf, S., Sellin, M., Fowler, A., Saunders, T., and
 471 Newman, S. J. (2015). Revolutionising Fish Ageing: Using Near Infrared Spectroscopy to Age
 472 Fish. Department of Agriculture, Fisheries and Forestry. Brisbane, April, 2015. CC BY 3.0.
- 473 Roggo, Y., Chalus, P., Maurer, L., Lema-Martinez, C., Edmond, A., and Jent, N. (2007). A
 474 review of near infrared spectroscopy and chemometrics in pharmaceutical technologies. *Journal*
 475 *of Pharmaceutical and Biomedical Analysis* **44**, 683-700.
- 476 Savitzky, A., and Golay, M. J. E. (1964). Smoothing and Differentiation of Data by Simplified
 477 Least Squares Procedures. *Analytical Chemistry* **36**, 1627-1639.
- 478 Shelton, A. O., and Mangel, M. (2012). Estimating von Bertalanffy parameters with individual
 479 and environmental variations in growth. *Journal of Biological Dynamics* **6**, 3-30.
- 480 Stokes, K., and Law, R. (2000). Fishing as an evolutionary force. *Marine Ecology Progress*
 481 *Series* **208**, 307-309.
- 482 Thompson, J. E. (2005). Age, Growth and Maturity of the Longnose Skate (*Raja rhina*) for the US
 483 West Coast and Sensitivity to Fishing Impacts. M.Sc. Thesis. State University, Oregon.
- 484 Vance, C.K., Tolleson, D.R., Kinoshita, K., Rodriguez, J., and Foley, W.J. (2016). Near infrared
 485 spectroscopy in wildlife and biodiversity. *Journal of Near Infrared Spectroscopy* **24**, 1-25.
- 486 Wold, S., Ruhe, A., Wold, H., and Dunn III, W. J. (1984). The collinearity problem in linear
 487 regression. The Partial least squares (PLS) approach to generalized inverses. *Society for*
 488 *Industrial and Applied Mathematics* **5**: 735-743.

RAPID AGE ESTIMATION OF LONGNOSE SKATE VERTEBRAE

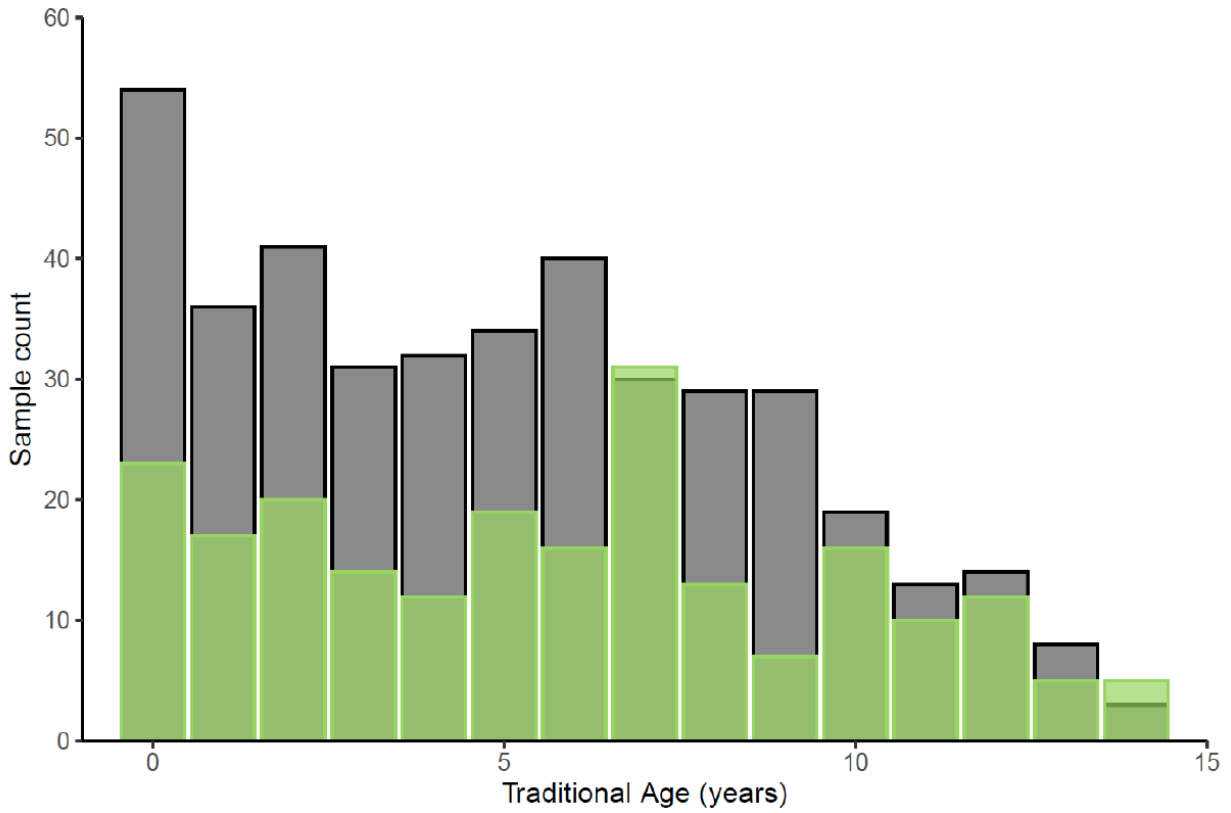
- 489 Wedding, B.B., Forrest, A.J., Wright, C., Grauf, S., Exley, P., and Poole, S. E. (2014). A novel
490 method for the age estimation of saddletail snapper (*Lutjanus malabaricus*) using Fourier
491 transform – near infrared (FT-NIR) spectroscopy. *Marine and Freshwater Research* **65**, 894-900.
- 492 Wright, C., Wedding, B.B., Grauf, S., and Whybird, O.J. (2021). Age estimation of barramundi
493 (*Lates calcarifer*) over multiple seasons from the southern Gulf of Carpentaria using FT-NIR
494 spectroscopy. *Marine and Freshwater Research*.

RAPID AGE ESTIMATION OF LONGNOSE SKATE VERTEBRAE

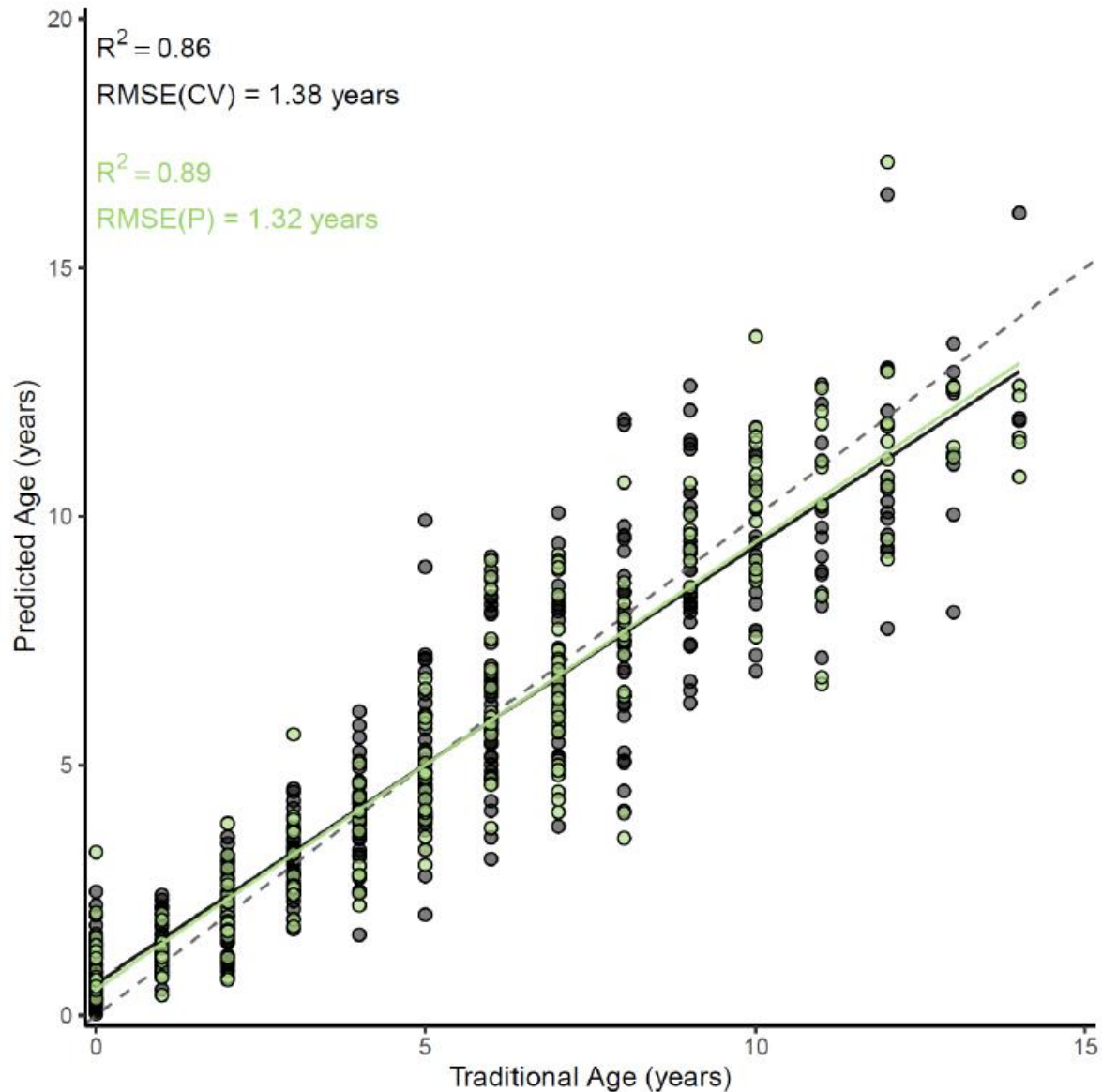


495 Figure 1. Fourier transform near infrared spectral absorbance data of all Longnose Skate
496 vertebrae. Spectra were averaged by traditionally estimated age, represented in colors: (A) raw
497 absorbance data and (B) pre-processed spectral data using a 1st derivative Savitzky-Golay
498 transform (17-point smooth, polynomial order = 1) and mean centering.

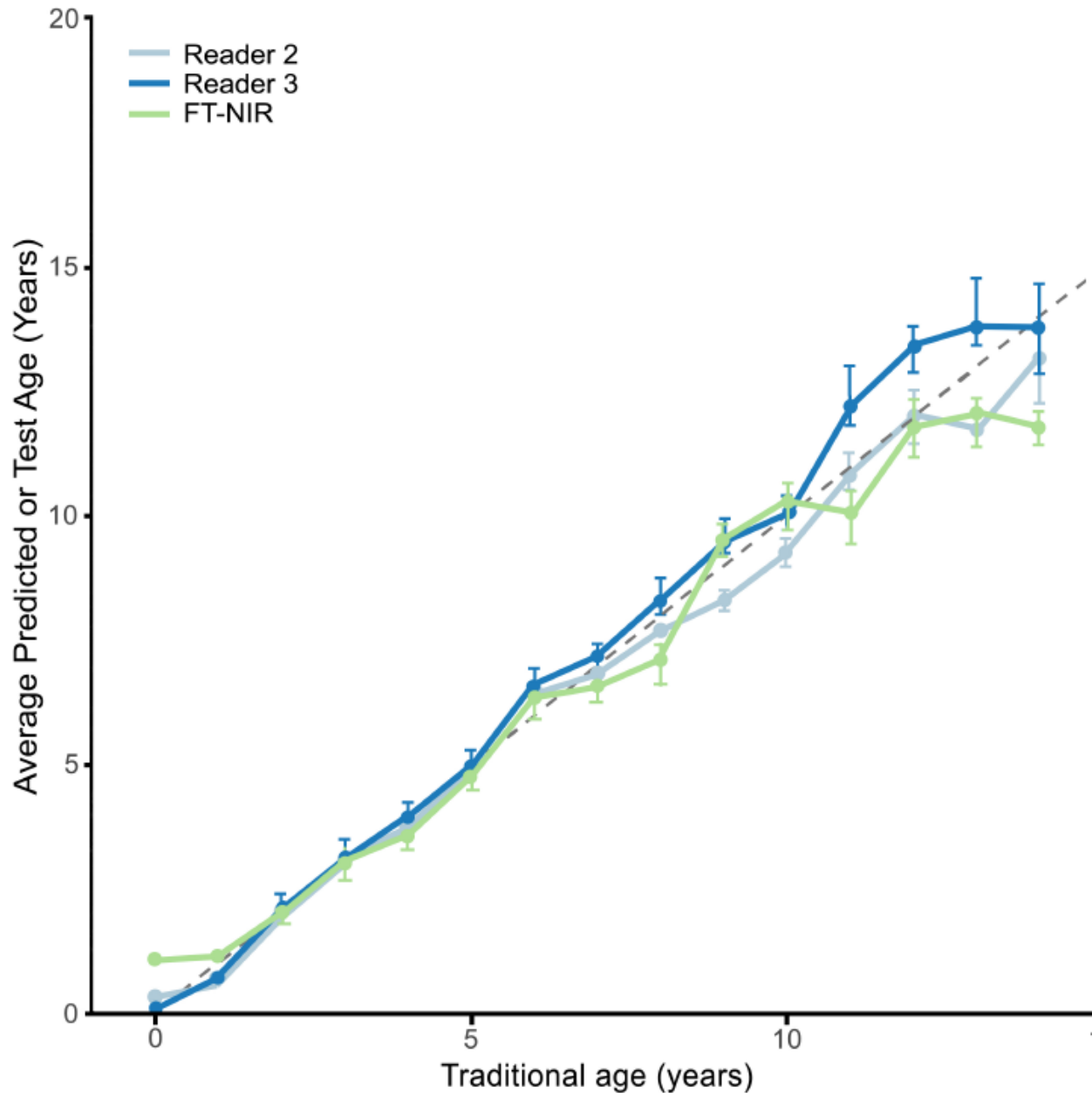
RAPID AGE ESTIMATION OF LONGNOSE SKATE VERTEBRAE



499 Figure 2. Age-specific sample sizes for the calibration set (grey) overlapped by external
500 validation set (green) used in the age estimation of longnose skate by Fourier transform near
501 infrared (FT-NIR) spectroscopy.

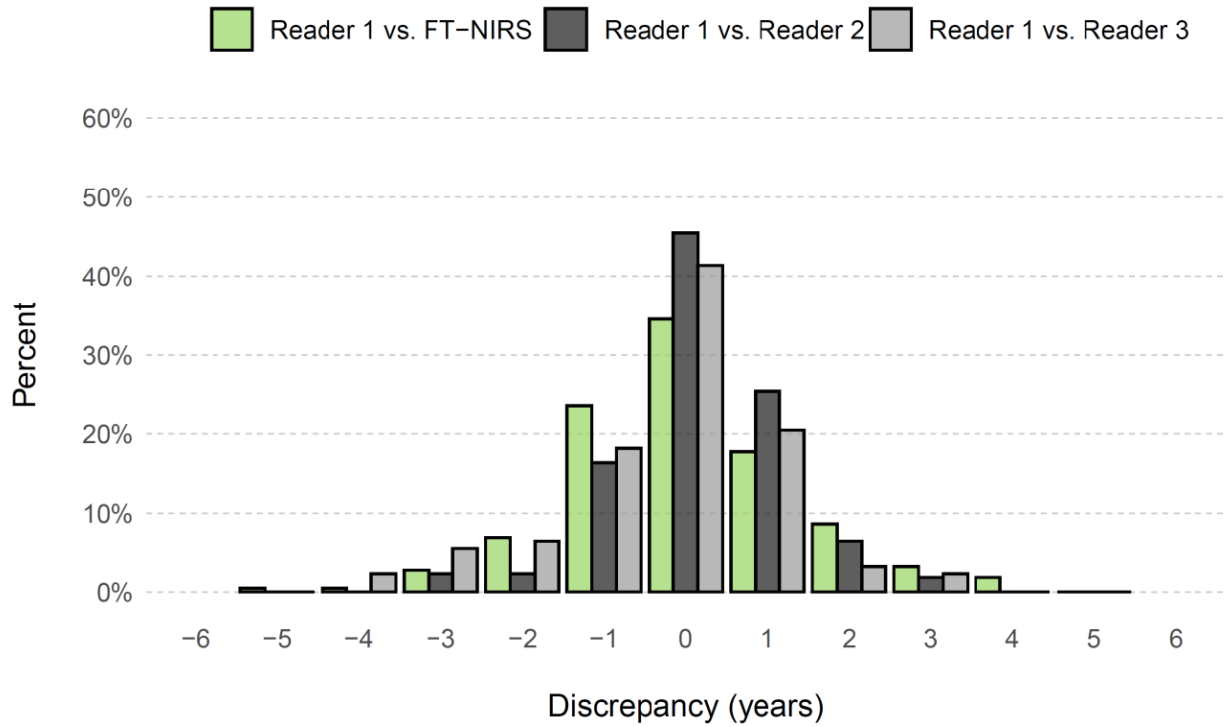


502 Figure 3. Results of a partial least squares model fit between reader-estimated age (traditional
 503 age) and Fourier transform near infrared spectra (predicted age) of Longnose Skate vertebral
 504 centra. Age predictions relative to traditionally estimated ages shown for the cross-validation
 505 (black) and for the external validation set (green) for each specimen. The solid lines are the
 506 regression lines for the cross-validation (black) and external validation (green). The dashed line
 507 represents one-to-one agreement between prediction and traditional estimate. Transparency in
 508 point shading shows overlapping data points.



509 Figure 4. Bias plot comparing Reader 1's traditional age estimates to: average age estimates of
 510 Reader 2 (light blue), Reader 3 (in dark blue) and Fourier transform near infrared (FT-NIR)
 511 predictions (green) for longnose skates. Standard error bars shown for age groups with multiple
 512 samples. Dashed line represents 1:1 agreement. Sample count for each age category are
 513 represented by grey bars.

RAPID AGE ESTIMATION OF LONGNOSE SKATE VERTEBRAE



514 Figure 5. Comparing discrepancies in longnose skate (*Raja rhina*) age estimates for the validation
 515 set from Fourier transform near infrared spectroscopy (FT-NIRS) and three age readers using
 516 traditional methods. Discrepancies are shown as percentage of specimens with age estimate
 517 differences of 0 to 6 years. In grey: traditional age estimated by Reader 1 – 2 and Reader 1 - 3,
 518 and in green: Reader 1 – FT-NIR prediction.